

# Indications of Spin-Charge Separation at Short Distance and Stripe Formation in the Extended t-J Model on Ladders and Planes

G. B. Martins<sup>1</sup>, J. C. Xavier<sup>1</sup>, C. Gazza<sup>2</sup>, M. Vojta<sup>3</sup>, and E. Dagotto<sup>1</sup>

<sup>1</sup> National High Magnetic Field Lab, Department of Physics,

and MARTECH, Florida State University, Tallahassee, FL 32306, USA

<sup>2</sup> Instituto de Física Rosario (CONICET) and Universidad Nacional de Rosario, 2000 Rosario, Argentina

<sup>3</sup> Department of Physics, Yale University, P.O. Box 208120, New Haven, CT 06520-8120, USA

(February 4, 2022)

The recently discussed tendency of holes to generate nontrivial spin environments in the extended two-dimensional t-J model (G. Martins, R. Eder, and E. Dagotto, Phys. Rev. B 60, R3716 (1999)) is here investigated using computational techniques applied to ladders with several number of legs. This tendency is studied also with the help of analytic spin-polaron approaches directly in two dimensions. Our main result is that the presence of robust antiferromagnetic correlations between spins located at both sides of a hole either along the x or y axis, observed before numerically on square clusters, is also found using ladders, as well as applying techniques based on a string-basis expansion. This so-called "across-the-hole" nontrivial structure exists even in the two-leg spin-gapped ladder system, and leads to an effective reduction in dimensionality and spin-charge separation at short-distances, with a concomitant drastic reduction in the quasiparticle (QP) weight  $Z$ . In general, it appears that holes tend to induce one-dimensional-like spin arrangements to improve their mobility. Using ladders it is also shown that the very small  $J/t \approx 0.1$  regime of the standard t-J model may be more realistic than anticipated in previous investigations, since such regime shares several properties with those found in the extended model at realistic couplings. Another goal of the present article is to provide additional information on the recently discussed tendencies to stripe formation and spin incommensurability reported for the extended t-J model. These tendencies are here illustrated with several examples.

PACS numbers: 74.20.-z, 74.20.Mn, 75.25.Dw

## I. INTRODUCTION

The study of high temperature superconductors continues attracting the attention of the Condensed Matter community. In recent years, much effort has been devoted to the understanding of the spin incommensurability that appears in neutron scattering experiments for some of these compounds [1]. Tranquada's interpretation of the experiments is based on "stripes" where charge is confined to one-dimensional (1D) paths in the crystal, with an average hole charge  $n_h = 0.5$ , namely one hole for every two sites along the stripe [1]. The stripe interpretation appears robust in the one-layer material  $\text{La}_{2-x}\text{Sr}_x\text{CuO}_4$ , although it is still controversial in the bilayer  $\text{YBa}_2\text{Cu}_3\text{O}_{6+x}$  [2]. Experimental results compatible with metallic stripes have also been reported using other techniques [3]. On the theory front, early studies discussed the presence of stripes in Hubbard and t-J models, although typically with density  $n_h = 1.0$  [4,5]. Recently, the existence of  $n_h < 1$  stripes was discussed using computational techniques directly in the t-J model at intermediate coupling  $J/t$ , without the need of long-range Coulomb interactions [6]. Sometimes these stripes are described as a condensation of d-wave pairs [7]. Stripes appear also in Monte Carlo studies of the spin-fermion model [8]. However, the origin of such complex spin-charge arrangement is still under much discussion, and

even its stabilization remains controversial in the standard t-J model [9].

In parallel with the developments in neutron scattering experiments, in recent years photoemission techniques have provided a plethora of information about the cuprates. In particular, the experimental study of the one-hole spectral function of the parent insulator compound gave us useful information to judge the quality of existing models for these materials [10]. Based on the experimental one-hole dispersion it has been convincingly shown that the t-J model is not enough to address the cuprates but extra terms must be added in order to reproduce the photoemission results for the insulator [11]. These terms appear in the form of extra hole hoppings, regulated in intensity by hopping amplitudes usually denoted by  $t^0$  and  $t^{\infty}$ . The bare value of these extra amplitudes is small compared with the nearest-neighbor hopping  $t$ , but its influence is substantial since they link sites belonging to the same sublattice and they are not so heavily renormalized to smaller values as it occurs with  $t$ . The origin of these extra hoppings was discussed before [11] and they appear naturally in mappings from the three-band model for cuprates to a one-band Hamiltonian, and also in band-structure calculations. In fact, what is unnatural is to assume that the standard t-J model, with  $t^0 = t^{\infty} = 0.0$ , is valid for the cuprates without corrections. Unlike in gauge theories, there are no

renormalizability or symmetry arguments at work preventing the introduction of nonzero extra hoppings in models for copper oxides. For these reasons it is important to study the extended t-J model in detail and, in particular, whether stripes occur in its ground state.

Recent studies of the extended t-J model have provided useful and sometimes surprising information [12,13]. For instance, it was observed that the one-hole QP weight  $Z$  is considerably reduced by the addition of  $t^0$  and  $t^{00}$  at fixed  $J/t$ . This result is particularly dramatic at momenta  $(0; \pi)$  and  $(\pi; 0)$ , and its origin lies in the generation of across-the-hole antiferromagnetic (AF) correlations, namely in the reference frame of the mobile hole the two spins immediately next to it along one axis are aligned antiferromagnetically [12]. This tendency is the opposite as expected from a vacancy in an antiferromagnet where those two spins should be ferromagnetically aligned, since they are in the same sublattice. Such a curious result was also observed in previous DMRG studies of ladders and planes using the standard t-J model by White and Scalapino [14]. Its importance and origin was recently discussed by Martins et al. [12] where its presence was conjectured to be caused by tendencies in the system to spin-charge separation at short distances. In other words, the kinetic energy of the hole with the extra mobility induced by  $t^0$  and  $t^{00}$  dominates most of the physics of the one-hole problem and it tries to generate in its vicinity an environment that allows for the hole to move without fighting against the spin background. In one-dimension this is easy to set up, and indeed an antiferromagnetic across-the-hole environment is stabilized on chains leading to spin-charge separation [15]. In two-dimensions the hole tries to create such an environment in its vicinity but it cannot produce a total spin-charge separation since frustration is induced when antiferromagnetic across-the-hole interactions are generated along both axes. It is expected that for realistic values of the couplings, the spin-charge separation will only be local (i.e. at short distances) [12]. This result, obtained using small square clusters [12], is clear in the presence of nonzero  $t^0$  and  $t^{00}$  of the proper sign and magnitude, but it also occurs in the standard t-J model in the regime of very small  $J/t$ , which remains mostly unexplored. This interesting observation redresses the relevant value of the parameter  $J/t$  from the number usually used in most studies (0.3-0.4) to smaller values close to 0.1.

Also motivated by the results in Ref. [12], recently the analysis of many holes at couplings that are expected to lead to robust across-the-hole correlations was reported by Martins et al. [13]. Indications of stripes were obtained in this case, similarly as those previously found in Ref. [6], rationalized as the natural tendency of locally spin-charge separated states to avoid the spin frustration caused by the nontrivial spin environment that each hole generates. The hole density in these stripes is in good agreement with experiments, and qualitatively the results resemble those in the "holons in a row" picture

of Zaanen [4]. Tight hole bound-states are not needed to generate stripes.

These observations suggest that either the extended t-J model or the standard t-J model at very small coupling must be analyzed in detail if the goal is to reproduce the physics of the striped regime of the cuprates. In addition, it is important to confirm the generality of previous results [12] by studying other systems with similar physics but where computational studies can be carried out on larger clusters. For this purpose, here ladders are investigated using the extended and standard t-J models in the coupling regime where in Ref. [12] the robust across-the-hole feature was observed on small square clusters. Our main result is that these robust correlations are also very clearly identified on ladders, even with only two legs, and, thus, its presence is more general than naively anticipated. Based on our results it is clear that holes on ladders tend to form one-dimensional (1D) like environments in their vicinity to improve their kinetic energy leading to an effective reduction in dimensionality. Spin incommensurability is generated by this procedure, a novel result in two-leg ladder systems to the best of our knowledge, although its presence in two dimensions has been known for some time [16].

The present paper has a second goal which is the detailed analysis of stripe formation upon doping of ladders with many holes. For this purpose here the recent results of Ref. [13] where stripes were observed are extended to couplings and parameters not reported before, to illustrate and confirm the tendencies toward stripe formation in this context. The proposed rationalization for this stripe stabilization was already discussed [13] and it is based on the sharing of the locally spin-charge separated spin environment created by each individual hole, thus avoiding spin frustrating effects.

The model used here is the extended t-J model defined as

$$H = \sum_{\langle ij \rangle} J (S_i \cdot S_j - \frac{1}{4} n_i n_j) + \sum_{im} t_{im} (c_i^\dagger c_m + h.c.); \quad (1)$$

where  $t_{im}$  is  $t$  for nearest-neighbors (NN),  $t^0$  for next NN, and  $t^{00}$  for next next NN sites, and zero otherwise. The scale of energy will be  $t = 1$  unless otherwise specified. The rest of the notation is standard. Comparison with PES experiments [10] showed that  $t^0 = -0.35$  and  $t^{00} = 0.25$  are relevant to explain PES data [11,12]. To simplify our studies the ratio  $t^0/t^{00}$  will be fixed to -1.4 in most of our analysis, although other ratios will be used in some cases. As numerical techniques, the Density Matrix Renormalization Group (DMRG) [6,17], Exact Diagonalization [16], and an algorithm using a small fraction of the ladder rung-basis (optimized reduced-basis approximation, or ORBA [18]) are here used. The paper is organized by the number of legs of the ladders considered, from two to six. Analytical results are discussed after the numerical methods, illustrating the appearance of tendencies toward across-the-hole antiferromagnetism

in two dimensional systems. In the last section it is concluded that the mostly unexplored extended t-J model contains interesting physics related to the cuprates, that deserves further work.

## II. TWO-LEG LADDERS:

### A. One Hole:

The present computational analysis of ladder systems starts with the two-leg ladder case. Previous literature has shown that in the absence of  $t^0$  and  $t^{\infty}$  hoppings, and at intermediate values of  $J$ , such as 0.4, one hole behaves as expected from a carrier in an antiferromagnet even if the ladder spin background has only short-range magnetic order [19]. In other words, a hole creates a spin distortion in its vicinity (spin polaron) and the one-hole ground state has a finite QP weight  $Z$ . Two of these spin polarons bind into a hole pair that leads to superconducting correlations upon further doping [19]. However, in this paper our goal is to analyze a region of parameter space not studied before, to the best of our knowledge, where the hole is expected to be substantially more mobile. For this purpose  $J$  is reduced to values between 0.1 and 0.2, still within the domain considered realistic in studies of the cuprates, and  $t^0, t^{\infty}$  are made nonzero and of the sign and magnitude as suggested by photoemission experiments. At such "small" values of  $J/t$ , the spin background no longer is expected to fully control the behavior of the hole but the spins have to arrange in such a way that the hole kinetic energy is optimized (but still without leading to a ferromagnetic state that may be the best configuration at  $J/t = 0.0$ ).

Consider first Exact Diagonalization results in the one-hole sector. In Fig.1a, the spin-spin correlations are shown for the case where the hole is projected on the (arbitrary) site indicated, from the full one-hole lowest-energy state with momentum  $k = (\pi, 0)$ , working at  $J = 0.2$ ,  $t^0 = -0.35$  and  $t^{\infty} = 0.25$ . It can be observed that at a distance of about three lattice spacings from the hole the spin correlations are similar to the ones expected for an undoped ladder, with robust antiferromagnetism along both the rungs and legs. However, in the vicinity of the hole the spin correlations are substantially altered. In this case the spins belonging to the same rungs are no longer strongly antiferromagnetically correlated and the system in the vicinity of the hole resembles a pair of weakly-coupled portions of a chain, one per leg. In this respect it appears that an "effective" transition from a two-leg ladder to 1D chains has occurred near the hole, a surprising result. Holes seem to optimize their energy by creating 1D environments in its vicinity. Note the presence of robust across-the-hole spin correlation on the upper leg of Fig.1a, which also appears in the exact solution of the 1D Hubbard model due to spin-charge separation. Fig.1a suggests that the spin associated to the hole

is spread uniformly in the 1D-like segment dynamically generated, and in this respect spin-charge separation occurs locally, as anticipated in the Introduction and as it was reported in Ref. [12] using small square clusters. Note in Fig.1a that the spin belonging to the same rung as the hole appears as "free" and there is a strong AF bond at distance of two lattice spacings across it, as it occurs across-the-hole.

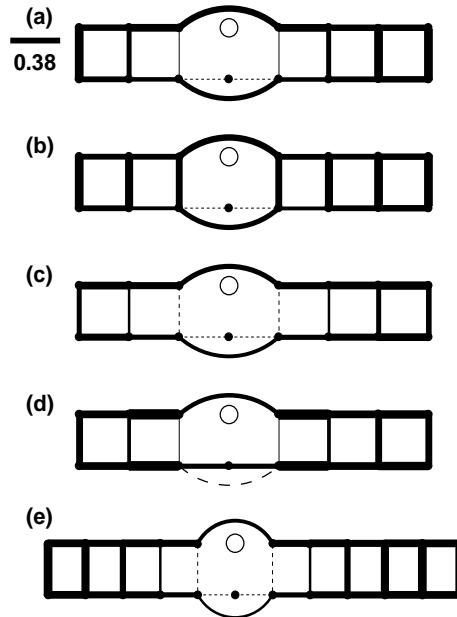


FIG. 1. Spin-spin correlations in the state with the lowest energy of one hole with momentum  $k$ , at the couplings described below. The data were obtained on the two-leg ladder using the Lanczos method on  $2 \times 8$  (a-d) and  $2 \times 12$  (e) clusters, with periodic boundary conditions (PBC) along the leg direction. Shown are results when the hole is projected from the state under consideration at the site indicated by an open circle. The dark lines between sites represent the absolute value of the (antiferromagnetic)  $\langle S_i \cdot S_j \rangle$  spin correlation between the spins located at those sites (scale shown in (a)). Dashed lines indicate weak ferromagnetic correlations. Results at distance of two lattice spacings are shown only near the hole. Note the presence of strong across-the-hole antiferromagnetic bonds in all the cases. (a) corresponds to  $J = 0.2$ ,  $t^0 = -0.35$ ,  $t^{\infty} = 0.25$  and  $k = (\pi, 0)$ . Far from the hole the spin correlations are as in undoped two-leg ladders, while near the hole they are much distorted, and they are robust mainly along the legs. (b) is the same as (a) but for  $t^0 = t^{\infty} = 0.0$ . (c) Results at  $J = 0.1$ ,  $t^0 = -0.35$ ,  $t^{\infty} = 0.25$  and  $k = (\pi, 0)$ . Note the appearance of some weak ferromagnetic rungs at this small value of  $J$ . (d) Same as (a) but for  $k = (\pi/2, 0)$ . (e) corresponds to  $J = 0.2$ ,  $t^0 = -0.35$ ,  $t^{\infty} = 0.25$  and  $k = (\pi, \pi)$ .

The comparison of Figs.1a and 1b, the latter obtained without extra hoppings, shows that  $t^0$  and  $t^{\infty}$  are important at  $J = 0.2$  to regulate the size of the 1D environment around the hole: as  $t^0, t^{\infty}$  grow in magnitude, the size of the 1D-like region also grows. This same effect is produced reducing  $J$  at fixed  $t^0, t^{\infty}$  as shown in Fig.1c: here

the distortion is larger than at  $J = 0.2$  and even weak ferromagnetic links are generated between the chains, an unexpected result quite different from the well-established physics of undoped ladders at intermediate  $J$ . The results here are also weakly dependent on the momentum: in Fig. 1d, the case of  $k = (\pi/2, 0)$  (momentum of the overall ground-state of one hole) presents a distortion similar in size as at  $k = (\pi, 0)$ , although the AF long-bond in the leg opposite to where the hole is projected (Fig. 1a) is no longer present. However, the long-bond across-the-hole is still robust. Fig. 1e is another case illustrating the momentum dependence in the problem, corresponding this time to  $k = (\pi, \pi)$ . Overall, it can be concluded that the lowest one-hole energy states for all momenta studied here, and in large regions of parameter space, present very similar spin arrangements. The across-the-hole feature emphasized in Ref. [12] is very robust in all cases and in this sense there is a clear shift across-the-hole even in the simple case of a two-leg ladder, similarly as it occurs in 2D systems. The dynamically induced 1D-like regions near the carrier are also clear in our studies.

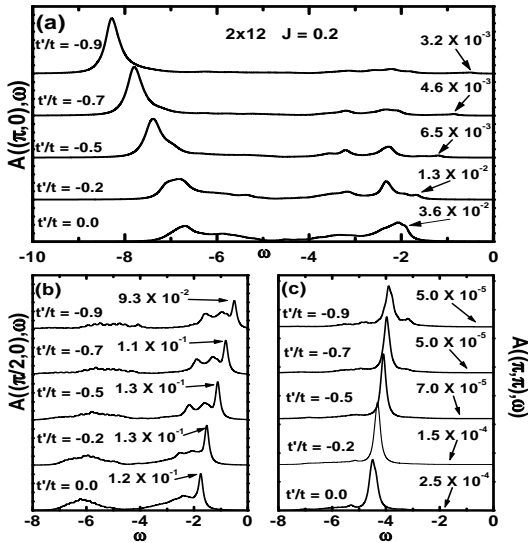


FIG. 2. One-hole spectral function  $A(k;!)$  obtained exactly from the undoped ground state of a  $2 \times 12$  cluster working at  $J = 0.2$ , and  $t^0 = -1.4t^{00}$  fixed, parametric with  $t^0$ . The arrows indicate the position of the first pole in the spectra and the numbers next to them are the weights  $Z$  (normalized such that  $0 \leq Z \leq 1$ ). (a) corresponds to  $k = (\pi, 0)$ , (b) to  $k = (\pi/2, 0)$ , and (c) to  $k = (\pi, \pi)$ .

The generation of a quasi-1D structure in the vicinity of the hole and the expected spread of the hole's spin-1/2 over several lattice spacings (spin-charge separation at short distances) causes a drastic reduction in the QP weight  $Z$ . In Fig. 2, the one-hole spectral function  $A(k;!)$  is presented at three different momenta. The results are shown as it is usual in experimental photoemission literature with the lower energy states appearing near  $! = 0$ ,

reference energy which is located at an arbitrary position in this half-filled case, and the rest of the states running to the left. Data for  $J = 0.2$  and several values of  $t^0$ , at fixed  $t^0/t^{00} = -1.4$ , are presented, together with the weight  $Z$  and position of the first state (arrows). Fig. 2a shows that  $Z$  at this value of  $J$  and  $k = (\pi, 0)$  is already small even in the absence of extra hoppings, result similar to those observed in previous investigations of the  $t$ - $J$  model on square lattices [16]. However, it is remarkable the rapid reduction of  $Z$  with increasing  $|t^0|$ , to values that in practice are basically negligible by the time these extra hoppings reach its realistic values. This is correlated with the appearance of the complex quasi-1D structure discussed in Fig. 1 [20]. A similar phenomenon but even more pronounced exists for  $k = (\pi, \pi)$  (Fig. 2c), where  $Z$  is negligible even without extra hoppings. On the other hand, the results at  $k = (\pi/2, 0)$  (Fig. 2b), while still corresponding to small values of  $Z$  of the order of 10% of the maximum, do not show such a dramatic reduction with increasing  $t^0$ . In this case the spin appears still located in the vicinity of the hole, although it is spread over several sites.  $Z$  becomes negligible at this momentum only at values of  $|t^0|$  larger than shown in the figure.

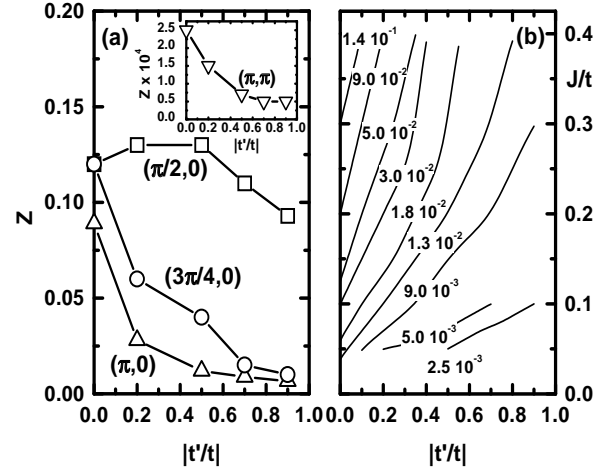


FIG. 3. (a) Weight  $Z$  of the lowest energy state in the  $A(k;!)$  one-hole spectral function of exactly solved  $2 \times 12$  clusters at  $J = 0.2$ ,  $t^0 = -1.4t^{00}$ , as a function of  $|t^0|/t$ .  $Z$  is normalized such that  $0 \leq Z \leq 1$ . Shown are results at the momenta indicated. In the inset the same information is given but for the nearly negligible lowest-pole weight of  $k = (\pi, \pi)$ . (b) Lines of constant  $Z$  weight (value indicated) in the plane  $J/t$  vs  $|t^0|/t$ , with  $t^0 = -1.4t^{00}$  fixed, corresponding to the lowest-energy pole in the  $k = (\pi, 0)$  subspace. Note the drastic reduction in  $Z$  as  $J$  is reduced from 0.4 and/or  $|t^0|$  is increased from 0.0. The results are interpolations using a fine grid of points obtained from the  $2 \times 8$  cluster solved exactly.

The results for the QP weight  $Z$  are more explicitly illustrated in Fig. 3a where its  $|t^0|$  dependence is shown for several momenta at fixed  $J = 0.2$ . Clearly for all momenta the presence of  $t^0$  eventually leads to a drastic reduction of the  $Z$  value, although for  $k = (\pi, 0)$  it happens

rapidly with increasing  $t^0$  while at  $k = (\pi, 0)$  it needs a  $t^0$  larger than the nearest-neighbors hopping  $t$ . In Fig.3b the lines of constant weight  $Z$  corresponding to  $k = (\pi, 0)$  are shown. It is clear that  $Z$  at this momentum rapidly reduces its value, both at fixed  $J$  increasing  $t^0$  or for fixed hoppings decreasing  $J$ . Although a careful finite size scaling is difficult, previous experience with two-dimensional clusters suggest that  $Z$  tends to decrease as the lattice size grows. As a consequence it is expected that the values reported in Figs.2 and 3 will actually be even smaller for a very long two-leg ladder. Note also that the lines of constant  $Z$  suggest that the physics of, say, intermediate  $J$  and finite  $t^0$  may be smoothly connected to that of small  $J$  and zero  $t^0$ , quite similarly as it happens on square clusters [12]. Then, it may occur that analyzing the regime of abnormally small  $J$  ( $< 0.1$ ) of the  $t$ - $J$  model may effectively account for the presence of extra hoppings, as was conjectured in Ref. [12]. This assumption is interesting due to the anticipated unusual properties of the small  $J/t$  region of the  $t$ - $J$  model, and it avoids the somewhat aesthetically unpleasant use of extra hoppings in the present theoretical studies.

#### B. Several holes:

The previous subsection showed that the two-leg ladder system presents exotic behavior in the one-hole sector when the regime of small  $J$  is investigated or alternatively when at a fixed  $J$  the hoppings  $t^0, t^y$  are switched on. It is important to explore what occurs for more holes in the problem, and Fig.4 contains exact results for the case of two holes on an  $2 \times 8$  ladder. Data is shown for the case when the two holes are projected to its most probable location in the ground-state, which in the cases studied coincide with the maximum distance among them allowed in the cluster. The spin structures in Fig.4 near the holes clearly resemble those found around individual holes in the previous subsection. In particular the across-the-hole AF correlation is very prominent in all cases shown in Fig.4. This structure naturally leads to spin incommensurability, as observed in the spin structure factor presented in Fig.5a [21]. It is interesting to observe that the coupling between chains can be weakly ferromagnetic in some cases (Fig.4a), weakly AF in others (Fig.4b), or even virtually negligible (Fig.4c) depending on the actual couplings used. Overall it is clear that the legs are approximately decoupled upon hole doping at the couplings analyzed here, and each leg behaves as a 1D-chain described by the same original  $t$ - $J$  model. Each individual leg resembles the expected result for the 1D Hubbard model at large  $U$  [15], as discussed before for 2D clusters [12]. It is remarkable that very recently nuclear spin relaxation results for two-leg ladder materials have also reported the decoupling of the two legs at high temperature [22]. The analysis of the relation between our results and those of Ref. [22] deserves further work.

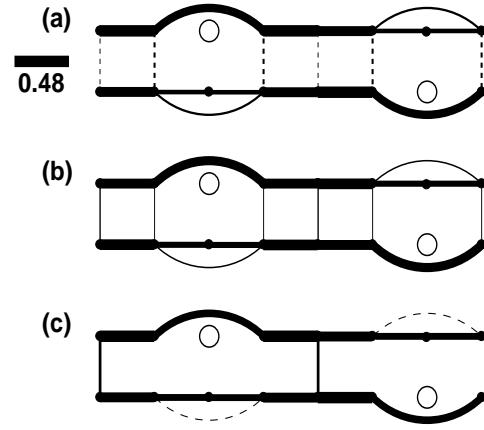


FIG. 4. Spin-spin correlations in the state with the lowest energy of two holes, at the couplings described below. The data were obtained exactly on the two-leg ladder using the Lanczos method on  $2 \times 8$  clusters with PBC along the legs. Shown are results when the holes are projected from the state under consideration at the sites indicated by open circles. These hole positions are the most probable in the two-holes ground-state. The dark lines between sites represent the strength of the antiferromagnetic spin correlation between the spins located at those sites (scale shown in (a)). Dashed lines indicate weak ferromagnetic correlations, and the missing vertical correlations indicate links with virtually negligible antiferromagnetic spin correlations. Results at distance of two lattice spacings are shown only near the hole. Note the presence of strong across-the-hole antiferromagnetic bonds in all the cases, as in the one-hole problem. Note also the clear tendency of spins in opposite legs to be nearly decorrelated. (a) corresponds to  $J = 0.2$ ,  $t^0 = -0.35$ , and  $t^y = 0.25$ . (b) corresponds to  $J = 0.2$ , and  $t^0 = t^y = 0.0$ . (c) corresponds to  $J = 0.4$ ,  $t^0 = -0.35$ , and  $t^y = 0.25$ .

In the two-hole ground-state the expectation value of the number operator for a particular momentum is shown in Fig.5b. Clearly the momenta  $k_x$  dominating in this state is not only  $\pi/2$ , the momentum of the lowest energy state of the one-hole sector, but actually  $3\pi/4$  and  $5\pi/4$  are also important as well as the  $k_y = \pi$  sector. Then, there is no indication of "hole-pockets" in the doped system, and momenta over a wide range contribute to the two-hole ground-state. This suggests that the one-hole states with the largest weight in the two-hole ground-state have the across-the-hole structure and local spin-charge separation.

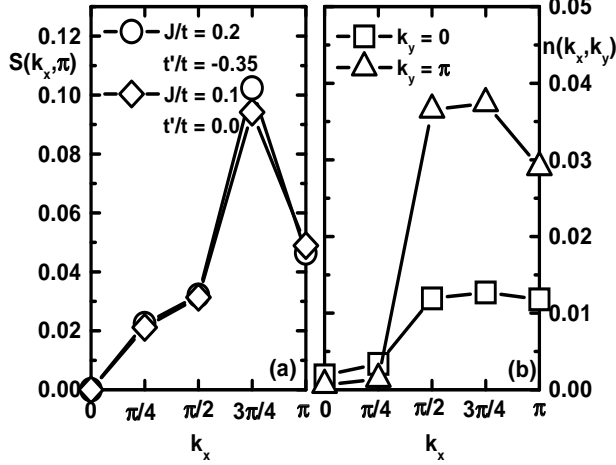


FIG. 5. (a) Spin structure factor  $S(k_x, k_y = \pi)$  vs  $k_x$  for the couplings  $J$  and  $t^0$  indicated (with  $t^0 = -1.4t^{\text{ex}}$ ), using the two holes ground-state of the  $2 \times 8$  cluster. Clear tendencies toward incommensurate correlations are observed in our study, as exemplified here, either at small  $J$  without  $t^0$  hoppings, or increasing the values of the latter at fixed  $J$ . (b) Exact  $n(k_x, k_y) = \frac{1}{N} \sum_j c_k^\dagger c_j$  vs  $k_x$  for the  $k_y$  momenta indicated, obtained using the ground-state of the two holes  $2 \times 8$  cluster and  $c_k = \frac{1}{N} \sum_j e^{ik \cdot j} c_j$ , where  $N$  is the number of sites in the cluster,  $j$  is a site index and  $k = \pm$ . The couplings are  $J = 0.2$ ,  $t^0 = -0.35$  and  $t^0 = 0.25$ .

The charge structure factor was also calculated in these investigations. In Figs. 6a-b exact results on a  $2 \times 8$  cluster and DMRG results on  $2 \times 16$  and  $2 \times 32$  clusters, all at hole density  $x = 0.125$ , are shown. They are very similar, illustrating the lack of strong size effects systematically observed in our studies of two-leg ladders. The results obtained in the more traditionally studied case of  $J = 0.4$ ,  $t^0 = t^{\text{ex}} = 0.0$  are also shown in Figs. 6c-d. They are qualitatively different from those in Figs. 6a-b, difference likely related with the formation of the quasi-1D regions mentioned before.

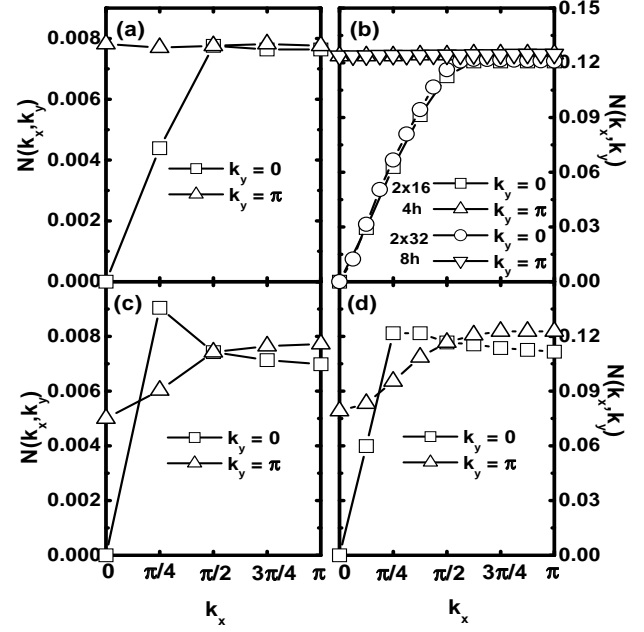


FIG. 6. Charge structure factor  $N(k_x, k_y)$  vs  $k_x$ , parametric with  $k_y$  as indicated. (a) corresponds to  $J = 0.2$ ,  $t^0 = -0.35$ , and  $t^{\text{ex}} = 0.25$  using the two holes ground-state of the  $2 \times 8$  cluster solved exactly. (b) Same as (a) but using  $2 \times 16$  and  $2 \times 32$  clusters and 4 and 8 holes, respectively, studied with the DMRG technique. (c) Same as (a) but for  $J = 0.4$ , and  $t^0 = t^{\text{ex}} = 0.0$ . (d) Same as (c) but on a  $2 \times 16$  cluster with 4 holes studied with the DMRG technique. Comparing (a) with (b), and (c) with (d), it appears that finite size effects are small.

### III. THREE-LEG LADDERS:

#### A. One hole:

Results for three-leg ladders have also been gathered in this work. In Fig. 7 the hole is projected at the location shown, from the lowest-energy state at the momenta indicated in the caption. In Fig. 7a results are presented at  $J = 0.1$  and nonzero  $t^0$ . The formation of the across-the-hole structure is very clear, in both directions. A long the vertical one, a strong AF bond is formed between the two spins of the rung where the hole is located. Its strength is close to that of a perfect singlet and, thus, the coupling of those spins with the rest is small. This structure is present at all the couplings investigated as shown in Figs. 7a-c, even intermediate and large  $J$ , and it is also clearly present in the exact solution of a three-site  $t$ - $J$  model at many couplings. In the small  $J/t$  regime of the standard  $t$ - $J$  model, and in the extended  $t$ - $J$  model as well, this strong AF bond denotes a precursor of the  $\pi$ -shift across the stripe that will form (along the PBC direction) as the hole-density increases. Regarding the horizontal AF bond (along the legs), its strength depends on the particular value of  $J$  and  $t^0$ . In the intermediate

coupling region often studied, exemplified by  $J=0.5$  and no extra hoppings as in Fig.7c, there is no across-the-hole AF correlation along the legs. On the other hand, for the couplings of Fig.7a, the clear 1D-like AF segment along the central leg induced in the vicinity of the hole suggests a larger mobility of the carrier and generation of 1D-like segments, as discussed in the Introduction and for two-leg ladders.

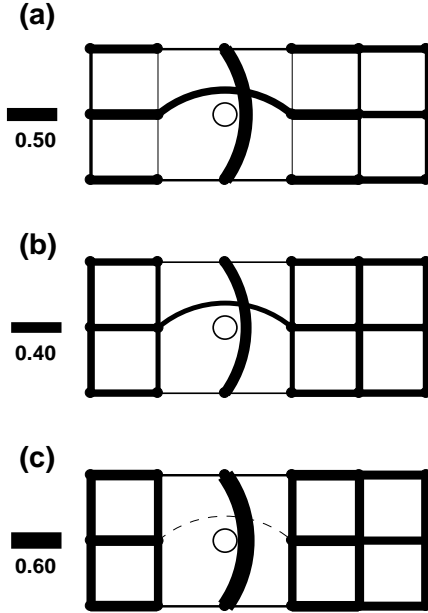


FIG. 7. Spin-spin correlations in the state with the lowest energy of one hole with momentum  $k$ , at the couplings described below. The data were obtained exactly on the three-leg ladder using the Lanczos method on  $3 \times 6$  clusters. PBC are used in the long direction and open boundary conditions (OBC) in the short one. Shown are results when the hole is projected at the site indicated by an open circle from the state under consideration. The dark lines between sites represent the absolute value of the (antiferromagnetic) spin correlation between the spins located at those sites (scale shown). The dashed line in (c) indicates a weak ferromagnetic correlation. Results at distance of two lattice spacings are shown only near the hole. (a) corresponds to  $k=(\pi/3, 0)$ ,  $J=0.1$ ,  $t^0=-0.35$ , and  $t^0=0.25$ . (b) corresponds to  $k=(\pi/3, \pi)$ ,  $J=0.1$ , and  $t^0=t^0=0.0$ . (c) corresponds to  $k=(\pi/3, \pi)$ ,  $J=0.5$ , and  $t^0=t^0=0.0$ .

The tendency toward local spin-charge separation can be studied further if the mean-value of the spin in the  $z$ -direction is calculated when the hole is projected from its ground-state to a given site, as done before in Figs.7a-c. Since removing one spin from a cluster with an even number of sites creates states with spin-1/2, together with the hole in Fig.8 there must be a spin-1/2 spread over the cluster. The results are shown in Fig.8a for the case of small  $J$  and nonzero  $t^0-t^0$ . In this situation it is clear that the  $z$ -component of the spin 1/2 is distributed approximately uniformly along the central leg where the hole is projected (the spin in the outer legs is negligible). In

agreement with the introductory discussion, the mobile hole creates a 1D environment (along the central leg in this case) to help in its propagation, and in this context the spin and charge are separated. On the other hand, the results corresponding to an intermediate  $J$  of value 0.5 and no extra hoppings corresponds to a staggered spin background surrounding the hole (Fig.8b), similar to results for a vacancy in a Neel background, with the exception of the two spins in the same rung as the hole, which try to form a strong singlet and thus its mean  $z$ -component spin tends to vanish. There is a clear qualitative difference between Figs.8a and b, caused by the high mobility of the hole in the presence of a small  $J$  and nonzero hoppings beyond nearest-neighbors. The QP weights  $Z$  (not shown) associated to the structure of Fig.8a tend to vanish at  $k=(0; \pi)$  and others, as found before for two-leg clusters and small two-dimensional systems.

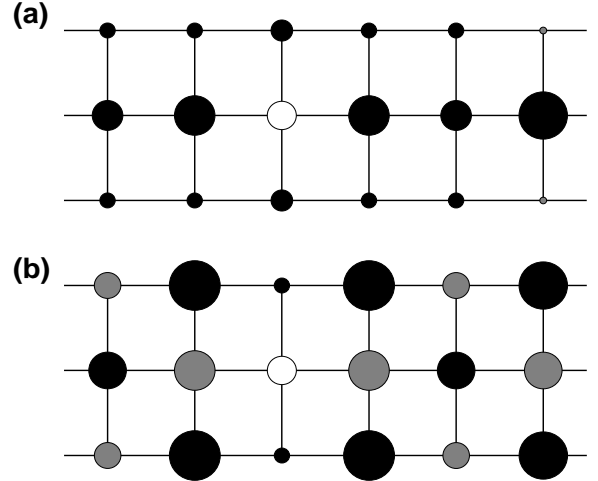


FIG. 8. Mean value of the  $z$ -component of the spin ( $\langle nS_z^2 \rangle$ ) denoted by the area of the circles, obtained from the one-hole ground-state of the  $3 \times 6$  cluster with the hole projected at the open circle position. Black (gray) circles indicate positive (negative) values. (a) corresponds to  $J=0.1$ ,  $t^0=-0.35$ , and  $t^0=0.25$ , while (b) corresponds to  $J=0.5$ ,  $t^0=t^0=0.0$ .

#### B. Many holes:

When two holes are considered on the three-leg ladder the situation is similar as in the case already described of two-legs, namely each individual hole carries a spin arrangement in its vicinity similar to that found in the one hole case. Results are shown in Fig.9a at small  $J$  and Fig.9b at intermediate  $J$ , in both cases without  $t^0-t^0$ . In the first case, AF bonds across-the-hole are found in both directions, while in the second the bond along the legs turns ferromagnetic as for vacancies in a Neel background and as in Fig.7c for one mobile hole [23].

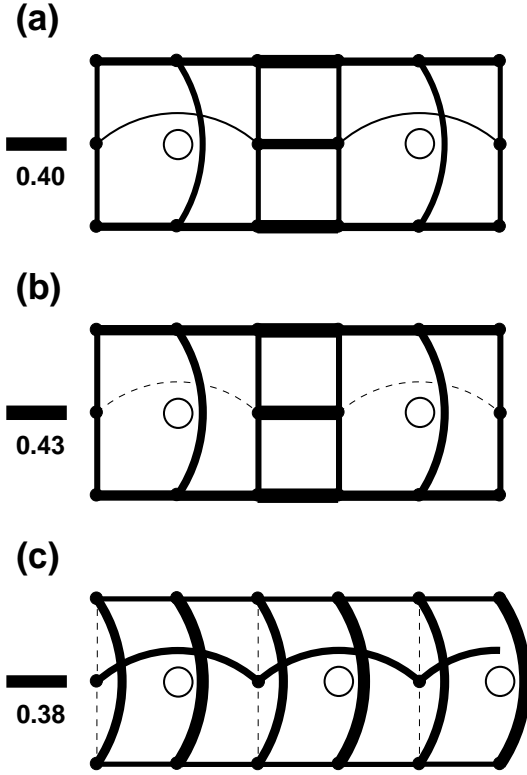


FIG. 9. Same convention as in Fig.7 but now for the two holes ground-state working at: (a)  $J=0.2$ , and  $t^0=t^00=0.0$ , and (b)  $J=0.5$ , and  $t^0=t^00=0.0$ . In this case the most likely configuration is a tight bound state (not shown). (c) Same as (a) but for the three holes ground-state at  $J=0.25$ ,  $t^0=-0.35$ ,  $t^00=0.25$ . In all cases the momentum is  $(0,0)$ .

If three holes are considered at small  $J$  (Fig.9c) the most likely hole configuration corresponds to a  $n_h=0.5$  stripe along the central leg, with clear and robust AF bonds across it joining the two outer legs (in spite of having open boundary conditions along the rungs). Within the central leg or stripe, AF bonds are formed across-the-hole, as in a 1D system with the same Hamiltonian. Fig.9c qualitatively indicates the dynamical separation of a chain subsystem carrying the charge from the rest of the spins which are correlated as if that chain would not exist. As emphasized in other parts of this paper and in Refs. [12,13], this appears to be the way in which the system achieves a partial separation of spin and charge in two dimensions.

#### IV. FOUR- AND SIX-LEG LADDERS:

##### A. One Hole:

Results similar to those found in the case of two- and three-leg ladders are also observed with four legs. Results for the case of one hole with momentum  $k=(\pi,0)$  are shown in Fig.10 on a  $4 \times 6$  cluster solved exactly using the Lanczos method. In Fig.10a results for small  $J$  and

nonzero  $t^0/t^00$  are presented: here the AF bonds across-the-hole can be observed and 1D-like segments are created near the hole in both directions [24]. The effect is amplified if at fixed  $J$  the values of the hoppings  $t^0/t^00$  are increased. Fig.10b contains the results using abnormally large extra hoppings: now the AF bonds across-the-hole are quite robust, with a strength that grows as the extra hoppings grow in magnitude. There is a smooth connection between the physically acceptable values of  $t^0/t^00$  and those used in Fig.10b to amplify the effect. Such a connection suggests a common origin to the structure.

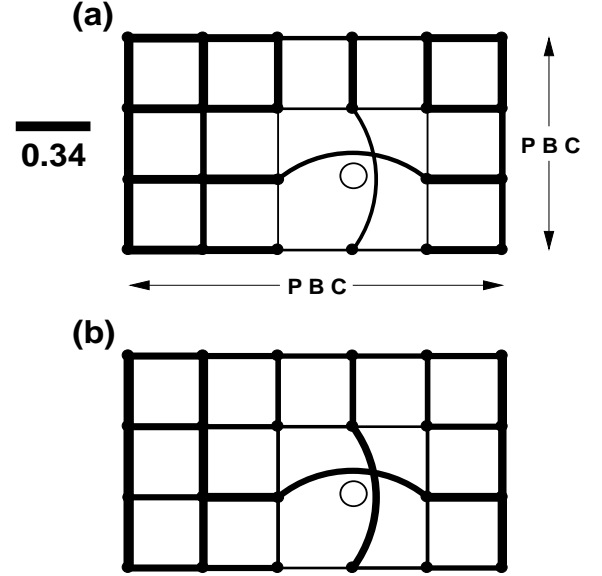


FIG. 10. Spin-spin correlations in the state with the lowest energy of one-hole with momentum  $k$ , at the couplings described below for a four-leg ladder. The data were obtained exactly using the Lanczos method on a  $4 \times 6$  cluster with PBC in both directions. Shown are results when the hole is projected at the site indicated by an open circle from the state under consideration. The dark lines between sites represent the strength of the antiferromagnetic spin correlation between the spins located at those sites (scale shown in (a)). Results at distance of two lattice spacings are shown only near the hole. (a) corresponds to  $J=0.2$ ,  $t^0=-0.35$ ,  $t^00=0.25$  and  $k=(\pi,0)$ . Far from the hole the spin correlations are as in undoped ladders, while near the hole they are much distorted. Note the clear presence of the across-the-hole antiferromagnetic bonds emphasized in this work. (b) Same as (a) but for  $t^0=-1.50$ ,  $t^00=1.07$  (keeping the same ratio  $t^0/t^00$  as in (a)). These large values of the extra hoppings are used to increase the magnitude of the effect.

The one-hole spectral function  $A(k; \omega)$  is shown in Figs.11a-b for the momenta indicated and as a function of  $\omega/t^0$ . At  $(0,0)$  the QP weight  $Z$  rapidly decreases with an increasing  $t^0$  hopping amplitude, while at a momentum closer to the expected ground-state momentum of one hole it remains more robust, but it eventually tends to vanish at large  $\omega/t^0$  (see also Fig.12). These results are very similar to those observed for two-leg ladders, for



planes [12], and also for three-leg ladders (not shown).

B. Many Holes:

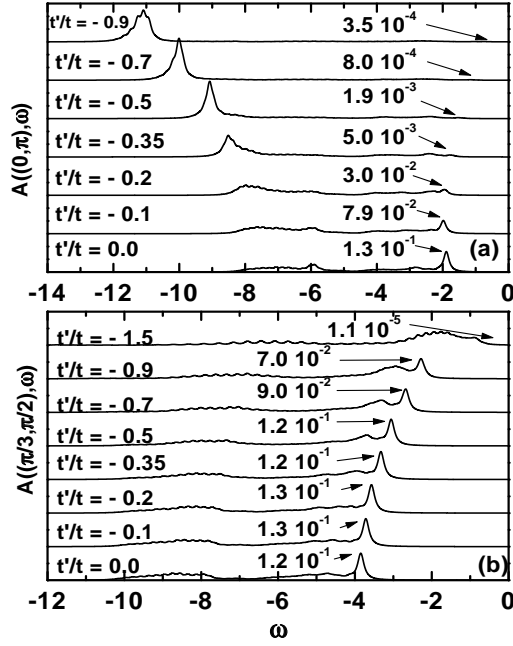


FIG. 11. One-hole spectral function  $A(k; \omega)$  obtained exactly from the undoped ground state of the 4x6 cluster with PBC in both directions, working at  $J=0.2$ , with  $t^0 = -1.4t^{\text{oo}}$  fixed, and parametric with  $t^0$ . The arrows indicate the position of the first pole in the spectra and its weight  $Z$  (normalized such that  $0 \leq Z \leq 1$ ). (a) corresponds to  $k = (0, \pi)$  and (b) to  $k = (\pi/3, \pi/2)$  (the closest to  $k = (\pi/2, \pi/2)$  in the cluster considered here).

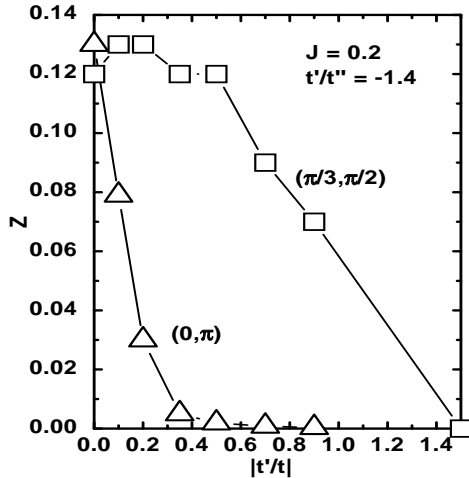


FIG. 12. Weight  $Z$  of the lowest energy state in the  $A(k; \omega)$  one-hole spectral function of exactly solved 4x6 clusters at  $J=0.2$ ,  $t^0 = -1.4t^{\text{oo}}$ , as a function of  $t^0/t_j$ .  $Z$  is normalized such that  $0 \leq Z \leq 1$ . Shown are results at the momenta indicated.

To clarify the behavior of two holes on four-leg ladders, consider the use of cylindrical boundary conditions (OBC in one direction and PBC in the other [6]). Suppose the two-hole ground-state is considered and one hole is projected to a site belonging to the central legs, where the density of holes is the largest. In this situation it is possible to study the probability of finding the other hole, with results shown in Fig.13a: the second hole clearly prefers to be along the PBC direction and still within the two central legs. Actually the largest probability is found at a distance of two lattice spacings along the same leg. The results can be interpreted as the formation of a loop of charge which wraps around the direction with PBC, as discussed recently in Ref. [13] and also in Ref. [6]. The state appears to correspond to a  $n_h = 0.5$  stripe, not rigid but fluctuating in the direction perpendicular to it.

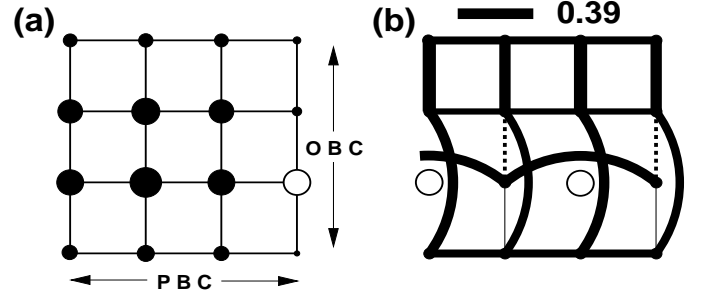


FIG. 13. Results corresponding to the exact two holes ground-state of a 4x4 cluster with PBC in one direction and OBC in the other, as indicated. The couplings are  $J=0.2$ ,  $t^0 = -0.35$ , and  $t^{\text{oo}} = 0.25$ . (a) corresponds to the case where one hole is projected from the ground-state into the location denoted by the open circle. The full circles have an area proportional to the probability of finding the second hole at a given site. A loop of mobile holes is dynamically formed around the PBC direction. (b) AF spin-spin correlations with the convention followed in previous figures, for the case where the two holes are projected from the ground-state at the location indicated by open circles. This hole configuration is the one with the largest weight in the ground-state. Results at distance of two lattice spacings are shown only near the stripe.

In Fig.13b the spin correlations are shown for the holes projected into the configuration with the largest weight in the two-hole ground-state. In agreement with the discussion associated with Fig.13a, the holes appear to be forming a  $n_h = 0.5$  stripe along the direction with PBC. Moreover, the spin correlations across-the-stripe are clearly antiferromagnetic as in the three-leg ladder (Fig.9c) and in experiments [1], and the two spins of the four-site stripe considered here are correlated also antiferromagnetically. This result is representative of a large number of similar data gathered in our present analysis, namely it appears that in general holes tend to form

loops of charge around the closed direction if a system has cylindrical boundary conditions. This is also in excellent agreement with the conclusions of earlier work by White and Scalapino [6], although their description of stripes is sometimes based on the condensation of d-wave pairs [7] while ours is based on a kinetic energy optimization (namely a one-hole problem).

The appearance of stripes based on the  $4 \times 4$  results of Fig.13 needs to be confirmed increasing the cluster size. This analysis was done in part in Ref. [13] as discussed in the Introduction, but here those results are expanded and more details are provided. Note that our present analysis using the DMRG method is restricted to the  $t$ - $J$ - $t^0$  model, namely the  $t^0$  hopping will be considered to be zero. The reason is that in the implementation of the DMRG technique sites are aligned along a one-dimensional pattern even for ladder geometries, and a  $t^0$  hopping would link sites along this equivalent chain which are located several lattice spacings from each other, reducing the accuracy of the method. Nevertheless even without  $t^0$  the stripes reported in Fig.13 and Ref. [13] can be clearly observed on larger systems. For example, consider in Fig.14 two holes on a  $4 \times 12$  cluster with cylindrical boundary conditions (PBC along the rungs),  $J=0.5$ , and  $t^0=-0.3$  ( $t^0=0.0$ ). One of the holes is projected to an arbitrary site of one of the central rungs, where the hole density is the largest. The distribution of the second hole around the projected one is quite similar to the result observed on the  $4 \times 4$  cluster, namely the largest chances are at distance of two lattice spacings along the rung. This state resembles a bound-state in the sense that the two holes are close to each other, but its shape is better described as a stripe configuration or a loop of charge that wraps around the short direction.

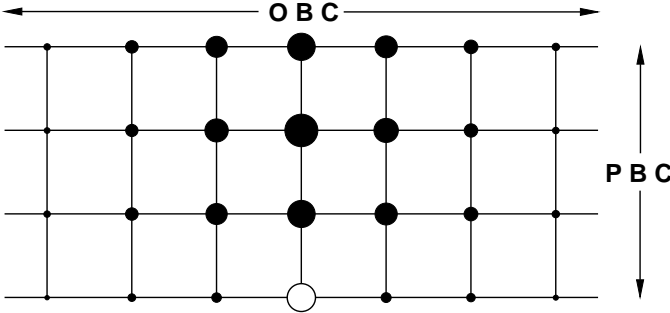


FIG. 14. Results corresponding to the two holes ground-state studied with the DMRG technique on a  $4 \times 12$  cluster with PBC in the short direction and OBC in the other, as indicated. The couplings are  $J=0.5$ ,  $t^0=-0.3$ , and  $t^0=0.0$ . One of the holes is projected at the open circle site. The full circles denote the probability of finding the second hole at a given site. A loop of mobile holes is formed wrapping around the rung direction.

If more holes are added to the four-leg ladder, it appears that stripes similar to those observed in Fig.14 are formed. For example, consider the case of four holes on

a  $4 \times 8$  cluster at small  $J$  and without  $t^0$  and  $t^0$ . In Fig.15 the density of holes is shown for the case where one hole is projected into one of the rungs with the largest density. It is clear from the figure that in the vicinity of the projected hole there is a structure similar to that observed for the two-hole ground state, namely a local maximum in the hole density is observed at two lattice spacings from the projected hole. In addition, clearly a large accumulation of charge appears on the other side of the cluster from where the projected hole is located. This other sector populated by holes involves two rungs in width, and it is framed in Fig.15. Note that the density in that second stripe is very uniform showing that there are no charge correlations between the two stripes (the two charged loops are independent of each other).

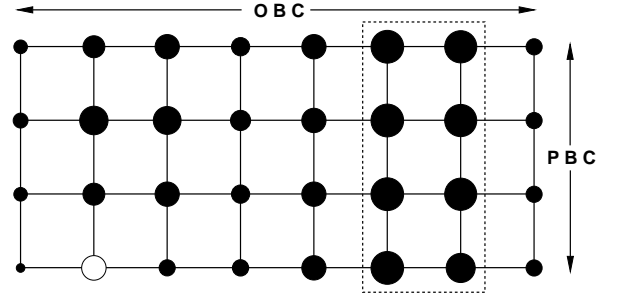


FIG. 15. Results corresponding to the four holes ground-state treated with the DMRG technique on a  $4 \times 8$  cluster with PBC in the short direction and OBC in the other, as indicated. The couplings are  $J=0.2$ , and  $t^0=t^0=0.0$ . One of the holes is projected at the open circle site. The full circles denote the probability of finding another hole at a given site. Two loops of mobile holes appear to be formed wrapping around the PBC direction (one of the two is framed).

In Fig.16a the charge structure factor is shown for the case of an  $4 \times 8$  cluster with four holes, studied with the DMRG method at small  $J$ . The result resembles those obtained for two-leg ladders in Fig.6. In Fig.16b the spin structure factor is shown for the same cluster and density. Spin incommensurability clearly appears in this system, as remarked before in Ref. [13] working at other couplings, and as presented for the two-leg ladder (Fig.5a) as well. It is clear that the two-, three- and four-leg ladder systems share very similar physics in the charge and spin sectors.

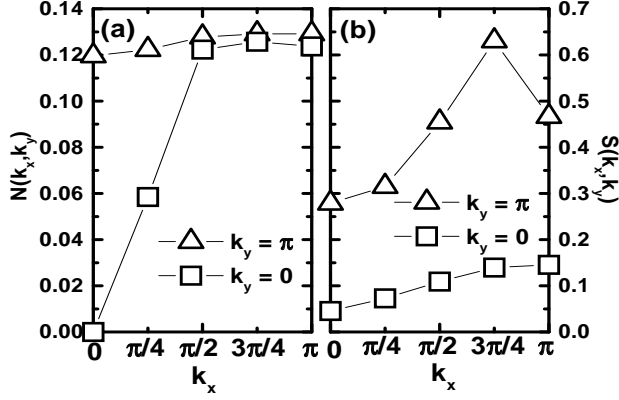


FIG. 16. Results obtained with the DMRG technique on a  $4 \times 8$  cluster with four holes ( $x=0.125$ ) at  $J=0.2$ , and  $t^0=t^{\pi}=0.0$ , using cylindrical boundary conditions (PBC along rungs). (a) Charge structure factor  $N(k_x, k_y)$  vs  $k_x$ , parametric with  $k_y$  as indicated. (b) Spin structure factor  $S(k_x, k_y)$  vs  $k_x$ , parametric with  $k_y$  as indicated. Incommensurability is clear in the  $k_y=0$  branch.

#### C. Six-leg Ladders:

Accurate results for six-leg ladders are difficult to obtain in the regime of parameters studied in this paper, namely small  $J$  and nonzero  $t^0, t^{\pi}$ . However, some non-trivial results can still be gathered. For instance, consider in Fig. 17 the case of three-holes on a  $6 \times 4$  cluster with PBC along the direction with six sites, and OBC along the short one. In this case a good approximation to the ground-state can be obtained using the ORBA method with about one million 4-site rung-basis states. The procedure to obtain the results shown in Fig. 17 are the following: first it was noticed that the central long legs are the ones most populated by holes. Then, one hole was projected at an arbitrary site belonging to those central legs. In the next step, the hole density is obtained with that hole projected, and at the position with the largest density a second hole is now projected. The distance between the first and second projected holes is two lattice spacings. With those holes projected as shown in Fig. 17, the hole density is recalculated. It is clear that at two lattice spacings from the projected holes the density has a maximum. This result is once again compatible with a  $n_h = 0.5$  stripe formed this time by three-holes in a closed loop around the direction with PBC. The stripe is not rigid but fluctuating perpendicular to its main direction.

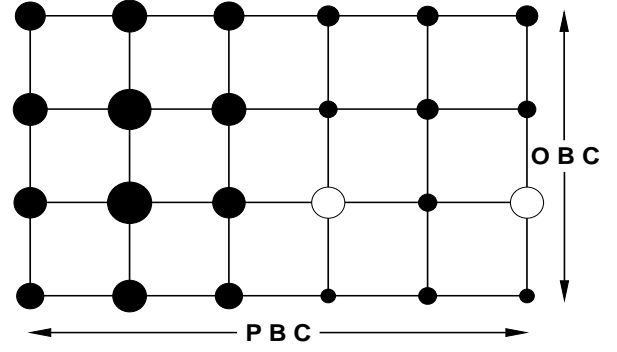


FIG. 17. Results corresponding to the three holes ground-state treated with the ORBA technique on a  $6 \times 4$  cluster with PBC in the long direction and OBC in the other, as indicated. The couplings are  $J=0.2$ ,  $t^0=-0.35$ , and  $t^{\pi}=0.25$ . Two of the holes are projected at the open circle sites. The full circles denote the probability of finding the third hole at a given site. A loop of mobile holes appears to form wrapping around the PBC direction.

The density of holes with a given momentum  $k$  for the  $6 \times 4$  cluster with three holes is shown in Fig. 18. Clearly the most important are those around  $(\pi, 0)$ , result similar to those reported for the two-legs cluster in Fig. 5b and for a  $4 \times 6$  two-holes cluster with PBC in both directions in Ref. [13].

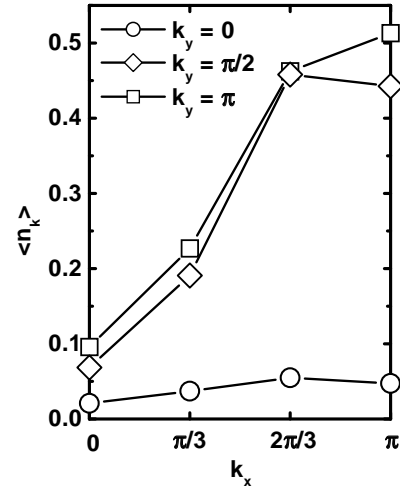


FIG. 18.  $n(k_x, k_y) = \frac{1}{N} \sum_j \langle c_{k,j}^\dagger c_j \rangle$  vs  $k_x$  for the  $k_y$  momenta indicated, obtained using the ORBA approximation to the ground-state of three holes on a  $6 \times 4$  cluster with PBC in the x-direction and OBC in the y-direction.  $c_k = \frac{1}{N} \sum_j e^{ik \cdot j} c_j$ , where  $N$  is the number of sites in the cluster,  $j$  is a site index and  $\pm = +; -$ .

## V. ANALYTICAL CALCULATIONS: SPIN-POLARON APPROACH

In previous sections, it has been shown among other items that the across-the-hole correlations identified before numerically on small square clusters for the one-hole problem [12] exist also on ladders. For completeness, in this section an analytical approach to the one-hole problem in two dimensions is described. In agreement with the above mentioned results, once again the existence of across-the-hole correlations is confirmed this time using a non-numerical method, highlighting the robustness of this feature.

The analytic approach used here is based on the picture of the spin-bag QP or magnetic polaron [25,28]. The spin deviations from a perfect antiferromagnet in the vicinity of the hole are described by a set of fluctuation operators  $A_n$  [25,27,28], which create strings of spin defects attached to the hole. The one-hole Green's function is evaluated using a cumulant version [29] of Mori-Zwanzig projection technique.

The undoped ground state is modeled by  $|j\rangle = \exp(\sum_n S_n^\dagger) |N_{\text{ee}}\rangle$  where the operators  $S$  create clusters of spin fluctuations in the classical Neel state. Following Ref. [30] it is possible to obtain a non-linear set of equations for the coefficients  $c_n$ , which is solved self-consistently. The fluctuation operators  $A_n$  for describing the spin deviations caused by hole motion include the usual string operators up to a certain length  $l_{\text{max}}$  and additional operators for local fluctuation configurations. The Green's function is calculated by projection technique in the subspace spanned by the operators  $A_n$ , which amounts to the diagonalization of the dynamical matrix  $h = \langle A_n^\dagger H A_n \rangle$ . Processes outside the subspace formed by  $A_n |j\rangle$  (i.e., self-energies) are neglected, therefore a discrete set of poles for each spectrum is obtained. The eigenvectors of the dynamical matrix represent the wavefunctions corresponding to the poles and they allow for the calculation of expectation values such as spin correlation functions. In the following the pole next to the Fermi surface representing the QP is the only one considered, the remaining part of the spectrum forms an incoherent background well separated from the QP peak. The approach sketched here has been successfully applied to the one-hole problem in several contexts [28,31]; details are described in Ref. [28]. In the present calculations strings with  $l_{\text{max}} = 5$  have been used (total number of fluctuation operators  $A_n$  around 1200). Note that the accuracy of the approximation decreases with increasing  $t$  since the employed expansion parameter is basically the amplitude of the deviations from the undoped state. Therefore it is better to restrict ourselves to the parameter range with  $J/t > 0.05$  where the comparison with numerical results reveals the good accuracy of the analytical approach.

First, let us discuss the weight of the QP pole which is known to decrease with decreasing  $J/t$  since the size

of the spin polaron increases. The full parameter dependence of the QP weight  $Z$  at momentum  $(\pi, 0)$  is shown in Fig. 19a. The introduction of  $t^0 < 0$  rapidly suppresses the value of  $Z_{\pi,0}$  even for intermediate or large  $J$ , such that the entire region of moderate  $t^0$  is characterized by small  $Z_{\pi,0}$ , in good agreement with the computational results shown in this paper and in Ref. [12]. On the other hand, the  $t^0$  dependence of  $Z$  at  $(\pi, \pi)$  is weaker (not shown), also as found in Ref. [12]. Nevertheless, its associated QP weight  $Z$  is also strongly suppressed with the reduction of  $J$ .

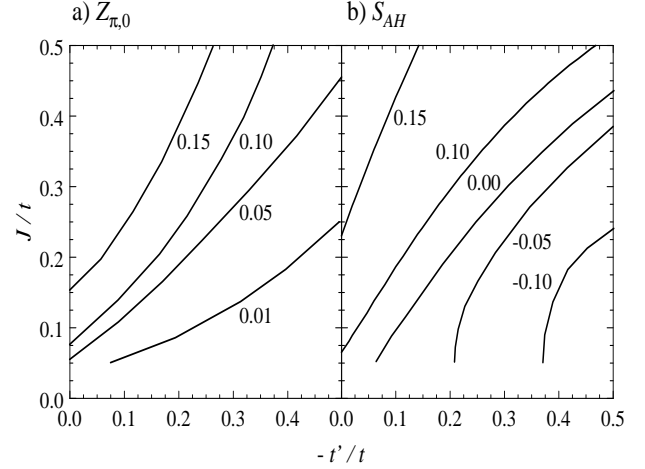


FIG. 19. (a) QP weight  $Z$  and (b) magnitude of across-the-hole correlations  $S_{AH}$  at momentum  $(\pi, 0)$  in the plane  $J/t$  vs.  $t^0/t$ , with  $t^0/t^0$  fixed to  $1/4$ .

In order to study the spin configuration near the mobile hole, static spin correlations in real space have been calculated relative to the hole position. It is known that the limit of small  $t$  (static vacancy) leads to an increase of the antiferromagnetic correlations on bonds near the hole, whereas hole hopping tends to "scramble" the spins in the hole environment which in general weakens the AF tendencies. This general behavior is well reproduced by our calculations. However, the introduction of  $t^0$  leads additionally to antiferromagnetic correlations  $S_{AH}$  across-the-hole, see Figs. 19b and 20b, quite consistent with those found numerically here and in previous studies. In Fig. 20b, the strength of the antiferromagnetic bonds at  $J = 0.05$ ,  $t^0 = -0.35$ ,  $t^0/t^0 = 0.25$ , and momentum  $(\pi, 0)$  are shown as illustration. A cross the mobile hole strong antiferromagnetic correlations develop which are supported by further strong AF bonds forming a chain segment. The other nearest-neighbor bonds are weaker by a factor of two than the chain bonds. The values of  $S_{AH}$ , obtained with the analytic approximation used in this section are shown in Fig. 19b. Although they are not as strong as found numerically, the qualitative trends agree quite well with computational studies.

The stronger tendency for local spin-charge separation, at small  $J/t$  or in the presence of  $t^0$  and  $t^0$ , can be un-

derstood within the string picture. The string of defect spins attached to the hole basically connects the spin and charge parts of the excitation, confining them at long distances. Therefore longer average strings correspond to less tightly bound spin and charge, i. e., larger spin polarons, immediately implying a smaller quasiparticle weight. The energy cost per unit length of string is proportional to  $J$ , hence smaller  $J/t$  allows for longer strings [25]. Interestingly, the presence of  $t^0$  and  $t^{00}$  leads to a related effect, namely the hole can easily 'get rid' of its attached string by intra-sublattice hopping, the string being then absorbed in the background spin fluctuations. This mechanism makes long strings effectively less costly, leading to the described large polarons with small QP weight  $Z$ .

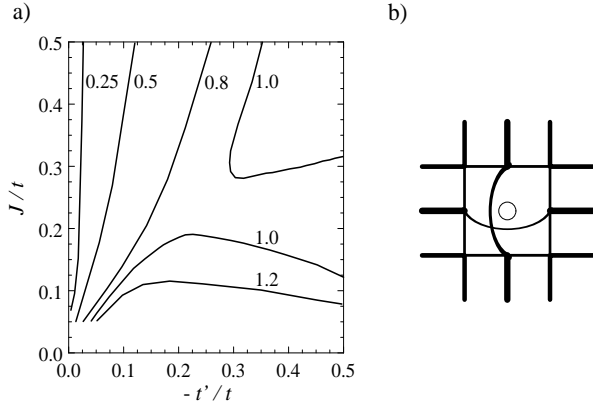


FIG. 20. (a) Ratio of the effective QP masses at momentum  $(\pi/2; \pi/2)$  which is a direct measure of the (an)isotropy of the dispersion. In the region near  $t^0=0$  and  $J/t=0.4$  the value is around 0.14 (in agreement with previous numerical studies [16]). (b) Illustration of the static spin correlations near the hole at  $J=0.05$ ,  $t^0=-0.35$ ,  $t^{00}=0.25$  and momentum  $(\pi/2; 0)$ . The width of the lines is proportional to the spin-spin correlation between sites  $i$  and  $j$ , namely  $\langle S_i S_j \rangle$ , and the value of the across-the-hole correlation is -0.1.

For completeness, in Fig 21 the calculated QP dispersions along high-symmetry lines in the Brillouin zone are shown. The points correspond to (a)  $J=0.40$ ,  $t^0=0.0$ , (b)  $J=0.40$ ,  $t^0=-0.35$  and (c)  $J=0.05$ ,  $t^0=-0.35$  with  $t^0/t^{00}=-1.4$ . The change in the curvature near  $(\pi/2; \pi/2)$  is clearly visible when adding  $t^0$  and decreasing  $J$ . Whereas the dispersion is strongly anisotropic for large  $J$  and small  $t^0$ , there is an entire region of near isotropy for moderate values of  $t^0$  and a large range of  $J/t$ , in agreement with PES experiments [10]. This is also illustrated in Fig 20a where the ratio of the effective QP masses at  $K_0=(\pi/2; \pi/2)$  for the entire parameter space are presented. The masses are defined as usual as eigenvalues of the tensor  $m_{ij} = \frac{1}{2m} \frac{\partial^2 E}{\partial k_i \partial k_j} (k=K_0)$  ( $k=K_0$ ) where  $k$  is the QP energy near  $K_0$ .

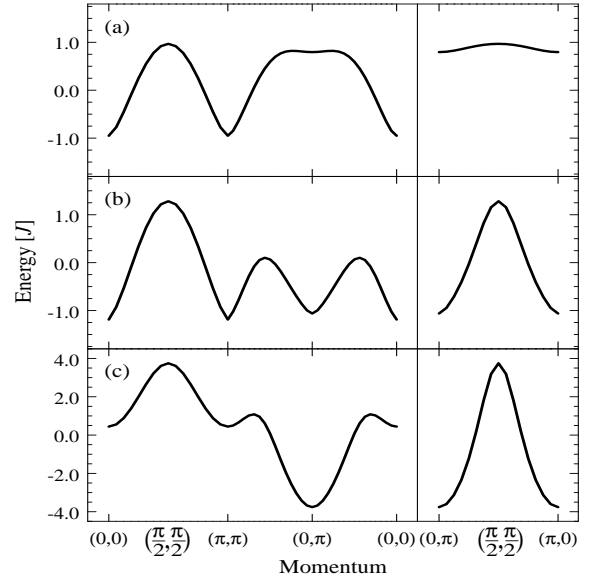


FIG. 21. QP dispersions for points (a), (b) and (c) as mentioned in the text. The energy zero level has been set at the center of mass of the band. The evolution towards a nearly isotropic maximum around  $(\pi/2; \pi/2)$  is clearly visible.

Summarizing, the introduction of  $t^0$  leads to a suppression of the QP weight, especially at momentum  $(\pi/2; 0)$ , a delocalization of the spin carried by the spin polaron, and the formation of antiferromagnetic correlations across the mobile hole. All the results are in good qualitative agreement with the numerical calculations reported here.

## VI. CONCLUSIONS

In this paper, tendencies toward spin-charge separation at short distances have been discussed in the context of the extended  $t$ - $J$  model using ladder geometries. This effort generalized previous calculations carried out on small square clusters. Analytic approximations have also been used, with results in good agreement with the computational ones. Overall it is concluded that in regimes where the hole kinetic part of the Hamiltonian dominates, holes tend to arrange the spin environment in such a way that across-the-hole robust antiferromagnetic correlations are generated, both on ladders and planes. This arrangement helps the hole move easily among the spins, and it resembles the structure found in one-dimensional spin-charge separated systems. For a variety of reasons described here, it is believed that at least at short distances similar tendencies toward spin-charge separation are at work in ladders and two-dimensional systems, at very small  $J$  in the standard  $t$ - $J$  model, or in the extended  $t$ - $J$  model. At finite hole density, holes share their nontrivial spin environment, forming half-doped stripes as recently discussed by some of the authors in Ref. [13]. Here more evidence substantiating this previous result has been pro-

vided. The stabilization of stripe tendencies discussed here is based upon a small  $J/t$  picture, and it has no obvious relation with those emerging in the opposite limit of large  $J/t$  based upon the frustration of phase separated tendencies. Although more work is certainly still needed to confirm the picture described here, it appears that a gas of spinons and holons, as envisioned in two-dimensional theories for cuprates based upon spin-charge separation, may not be operative at low hole densities, but instead stripes of holons seem to be forming.

## V II. ACKNOWLEDGMENTS

E. D. thanks NSF (DMR-9814350) and the Center for Materials Research and Technology (MARTECH) for support, J. C. X. thanks FAPESP-Brazil for support and C. G. thanks Fundacion Antorchas for partial support. M. V. acknowledges support by the DFG (VO 794/1-1) and by US NSF Grant DMR 96-23181.

- 
- [1] J. M. Tranquada et al., *Nature* 375, 561 (1995).
  - [2] H. A. Mook et al., *Nature* 395, 580 (1998); P. Dai et al., *Phys. Rev. Lett.* 80, 1738 (1998); P. Bourges et al., *Science* 288, 1234 (2000).
  - [3] N. Ichikawa et al., *cond-mat/9910037*.
  - [4] J. Zaanen, *J. Phys. Chem. Solids* 59, 1769 (1998).
  - [5] U. Low et al., *Phys. Rev. Lett.* 72, 1918 (1994); V. Emery et al., *Phys. Rev. B* 56, 6120 (1997). See also J. Zaanen and O. Gunnarsson, *Phys. Rev. B* 40, 7391 (1989); P. Prelovsek and X. Zotos, *Phys. Rev. B* 47, 5984 (1993); B. Stojkovic et al., *Phys. Rev. Lett.* 82, 4679 (1999).
  - [6] S. White and D. Scalapino, *Phys. Rev. Lett.* 80, 1272 (1998); *cond-mat/9907301*.
  - [7] S. White and D. Scalapino, *cond-mat/9610104*.
  - [8] C. Buhler, S. Yunoki and A. Moreo, *Phys. Rev. Lett.* 84, 2690 (2000).
  - [9] C. Hellberg and E. Manousakis, *Phys. Rev. Lett.* 83, 132 (1999); S. White and D. Scalapino, *ibid*, 84, 3021 (2000); M. Calandra and S. Sorella, *cond-mat/9911478*.
  - [10] F. Ronning et al., *Science* 282, 2067 (1998), and references therein.
  - [11] A. Nazarenko et al., *Phys. Rev. B* 51, 8676 (1995); V. I. Belinicher et al., *Phys. Rev. B* 54, 14914 (1996); R. Eder et al., *Phys. Rev. B* 55, R3414 (1997); F. Lema and A. Alogia, *Phys. Rev. B* 55, 14092 (1997). C. Kim et al., *Phys. Rev. Lett.* 80, 4245 (1998).
  - [12] G. Martins, R. Eder, and E. Dagotto, *Phys. Rev. B* 60, R3716 (1999).
  - [13] G. Martins, C. Gazza, J. C. Xavier, A. Feiguin, and E. Dagotto, *Phys. Rev. Lett.* 84, 5844 (2000).
  - [14] S. White and D. Scalapino, *Phys. Rev. B* 55, 6504 (1997).
  - [15] M. Ogata and H. Shiba, *Phys. Rev. B* 41, 2326 (1990).
  - [16] E. Dagotto, *Rev. Mod. Phys.* 66, 763 (1994).
  - [17] The truncation error was  $10^{-5}$  (keeping up to 800 states).
  - [18] E. Dagotto et al., *Phys. Rev. B* 58, 12063 (1998). See also J. Riera and E. Dagotto, *Phys. Rev. B* 47, 15346 (1993).
  - [19] E. Dagotto and T. M. Rice, *Science* 271, 618 (1996).
  - [20] Similar results but for  $k = (0; \pi)$  were shown in Ref. [13].
  - [21] For results at other couplings see Ref. [13].
  - [22] S. Fujiyama, M. Takigawa, N. Motoyama, H. Eisaki and S. Uchida, *cond-mat/0004433*, preprint.
  - [23] Results at small  $J$  and nonzero  $t^0 t^0$  were shown in Ref. [13] and there the inclusion of extra hoppings increased even further the across-the-hole correlations along the leg direction.
  - [24] Results at  $k = (\pi; \pi)$  can be found in Ref. [13].
  - [25] Y. Nagaoka, *Phys. Rev.* 147, 392 (1966); W. F. Brinkman and T. M. Rice, *Phys. Rev. B* 2, 1324 (1970); B. I. Shraiman and E. D. Siggia, *Phys. Rev. Lett.* 60, 740 (1988); S. A. Trugman, *Phys. Rev. B* 37, 1597 (1988).
  - [26] G. Martinez and P. Horsch, *Phys. Rev. B* 44, 317 (1991).
  - [27] J. A. Riera and E. Dagotto, *Phys. Rev. B* 55, 14543 (1997).
  - [28] M. Voja and K. W. Becker, *Phys. Rev. B* 57, 3099 (1998).
  - [29] K. W. Becker and W. Brenig, *Z. Phys. B* 79, 195 (1990).
  - [30] T. Schork and P. Fulde, *J. Chem. Phys.* 97, 9195 (1992).
  - [31] M. Voja, *Phys. Rev. B* 59 6027 (1999); M. Voja and K. W. Becker, *Phys. Rev. B* 60, 15201 (1999); M. Voja, *Phys. Rev. B* 61, 11309 (2000).